© 2007 OSA/NLO 2007

Overcoming traditional manufacturing limitations in high Q micro-ring resonators using non-linear effects in silicon

Michael Schmidt, Qianfan Xu, Michal Lipson, Hod Lipson
*School of Engineering, Cornell University**
mds47@cornell.edu , qx23@cornell.edu, lipson@ece.cornell.edu, hod.lipson@cornell.edu

Abstract: High sensitivity to fabrication errors is a main challenge in using high-Q resonators. Here we show that by carefully choosing the optical tuning using an evolutionary algorithm, a drastically distorted transmission function can be restored.

High Q ring resonators have been shown to enable novel functionalities on chip[1,2], however the main challenge in using high Q resonators is their high sensitivity to fabrication errors. These errors affect the dimensions of all the parameters of the resonator such as its radius, its quality factor Q and its resonance wavelength. As a results complex transmission functions, that are obtained by coupling such resonators are then drastically distorted.

Here we show that solely by choosing carefully the degree of tuning of the resonators, i.e., its resonance wavelength, a drastically distorted transmission function (due to variations in all of its geometrical parameters) can be recovered. The resonance wavelength of ring resonators can be tuned in silicon using all-optical modulation of the effective index induced due to two photon absorption, as recently demonstrated in ref. 5 and 6. Here the degree of tuning of each ring's resonances is determined by applying an optimization algorithm to the system.

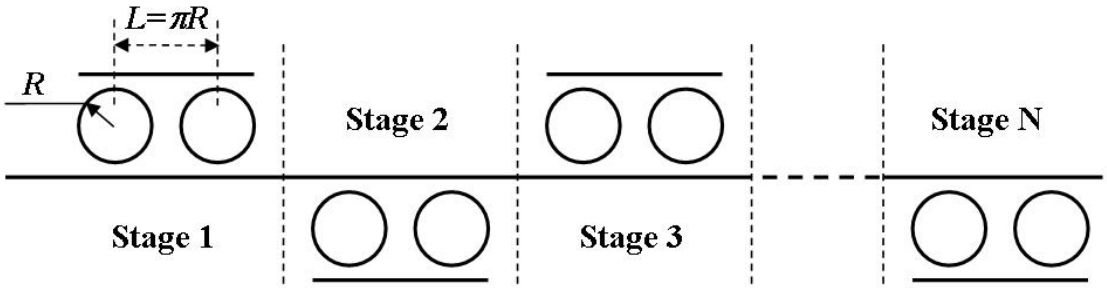


Fig. 1. Device structure.

The structure analyzed is shown in Fig. 1. Each stage of the device is a double-ring resonator. It consists of a pair of silicon ring resonators coupled to a pair of parallel silicon strip waveguides. The double-ring resonator has a sharp transmission line (EIT-like mode) resulting from a mode due to the interference between the two ring resonators [3]. By tuning the resonance wavelength of each resonator in the pair, one can control the effective-Q of this mode providing a high degree of freedom to tailor the spectrum. The structure of each stage of the device is defined by the parameters listed in Table I. The range of each parameter corresponds to the one that is typically achieved experimentally in such structures [4]:

Variable	Restricted Range
κ	0.0 – 1.0
α	0.0 – 0.005
Φ_0	0 - 2π
Φ_1	0 - 2π
Φ_2	0 - 2π
R	3000 – 10000 nm

Table I. Range of parameters describing each doubled ring resonator. The parameters controlled externally by all-optical effects are ϕ_1 and ϕ_2 shown in bold

© 2007 OSA/NLO 2007

R is the nominal radius of each ring resonator. κ is the field coupling coefficient between the waveguide and each ring resonator. It is defined as the amplitude of electric field coupled into the ring divided by the amplitude of electric field in the input waveguide. Its value is between 0 and 1. α is the field loss per round in the ring. Due to the optical scattering, the amplitude of electrical field drops to $e^{-\alpha}$ of the original amplitude after it pass one round in the ring. For example $\alpha = 0.003$ for a ring resonator with radius of 5 microns corresponds to an intrinsic Q of 91,000 for each ring resonator. ϕ_0 describes the deviation of the real distance between the two rings from the nominal distance πR, as defined in Fig. 1. ϕ_1 and ϕ_2 are defined as the phase shift per round in a ring with radius R for the light at the wavelength of λ_1 and λ_2, respectively. Since the resonant wavelength of each ring resonator depends on the effective index of the ring, ϕ_1 and ϕ_2 can be tuned at real time using nonlinear effects in silicon from 0 to 2π using for example low power external beams that are incident on the rings for injecting free carriers.

Variable	Device #1	Device #2	Device #3
κ	0.5785	0.6765	0.6807
α	0.0003253	0.002216	1.165e-5
Φ_0	3.9812	5.982	2.011
Φ_1	5.639	2.2582	4.0312
Φ_2	5.482	5.481	4.647
R	8731	7217	8628

Table II. The parameters for the ring device with transmission function shown in Figure 2 as the dotted line. We simulate manufacturing errors on this device by adding 10% random errors to all parameters. The damaged transmission function is shown in Figure 2 as a dashed line.

The transmission response of such structure depends strongly on the parameters in Table I. An example of such a spectrum is shown in Fig. 2 (dotted line) for three rings with parameters listed in Table II. In this paper, we simulate manufacturing errors by randomly off setting all parameters of each device by 10% of their range. As seen Figure 2,(dashed line) such small errors to all devices can drastically change the filter transmission.

In order to compensate for the variation in all the parameters we use an evolutionary algorithm to determine the tuning of only the parameters Φ_1 and Φ_2, in each ring (the ones that can indeed be controlled externally by injecting carriers using for example two photon abosprption induced by another beam of light incident on the ring [5,6]) that lead to a transmission spectrum that is very close to the original one. An evolutionary algorithm is a population-based optimization algorithm where initially random candidate solutions compete to maximize some heuristic [7]. The algorithm utilizes stochastic operations inspired by biological evolution – such as mutation, recombination, and selection – to synthesize new candidates and search for optimal solutions. Each iteration of the algorithm, or generation, generates a successive population by selecting, crossing, and mutating individuals from the previous population. The selection process picks individuals which perform the best to be crossed and recombined with other individuals to create offspring for the next generation. To measure the performance of each candidate filter [9] we define the degree of variation between the original transmission spectrum and the deformed filter by the mean-squared-error:

$$MSE = \sum_i \left(T(\lambda_i)' - T(\lambda_i)\right)^2$$

where the summation is over a set of training data (a range of wavelengths), $T(\lambda_i)'$ is the transmission of the damaged filter, and $T(\lambda_i)$ is the transmission of the designed filter. Solutions with low error (high fitness) are selected [8] to survive in the population or and to generate new solutions while high error solutions are rejected or replaced. The best candidate solution in the population is tracked over each generation to measure the algorithm's progress. Eventually, the performance of the best solution plateaus after several iterations and the solution is returned. Candidate filter solutions are encoded as a list of parameters for each device (up to 10) of the ring series. New solutions are formed by crossing two low-error solutions in the current population to randomly recombine their parameters. New solutions are also formed by mutation – randomizing some parameters in the filter.

© 2007 OSA/NLO 2007

The qualitative box-filter behavior (shown in Fig. 2 as solid line) is fully restored in the recovery stage by readjusting solely the Φ_1 and Φ_2 parameters. Note that some precision is lost. This result however shows that the dynamic parameters Φ_1 and Φ_2 alone are powerful enough to restore significant defects. Fig. 3 describes the remaining error (i.e., distortion of the transmission function) as a function of number of generation for which the algorithm is run. One can see that after 10^3 generations, which corresponds to approximately 5 min of computational efforts on a 3GHz machine, a very small mean square error is achieved.

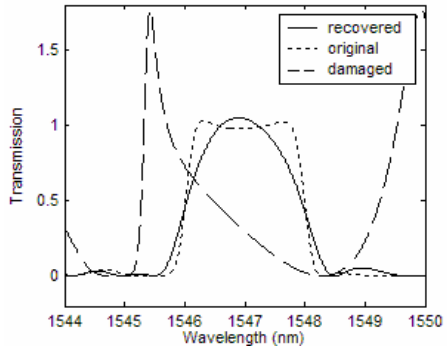


Fig. 2. A damaged five-device filter. *The* κ, α, Φ_0, R, and G parameters are offset by 10% random manufacturing error. The qualitative box-filter transmission function has been restored .

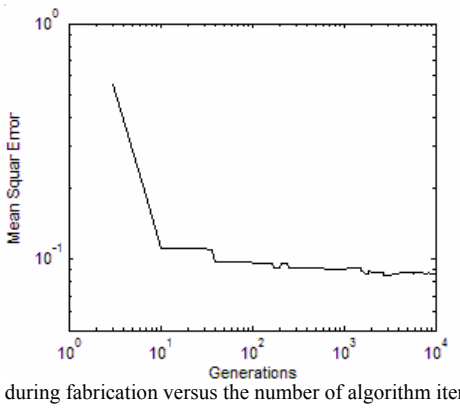


Fig. 3. Recovery of a ring series damaged during fabrication versus the number of algorithm iterations. The algorithm exploits the nonlinear influence of dynamic parameters o1 and o2 to reduce error resulting from manufacturing precision and restore intended functionality.

In conclusion we have shown the ability to overcome manufacturing variations and recover the intended functionality by determining the parameters that can be controlled externally using all-optical effects

[1] Q. Xu, and M. Lipson, "All-optical logic based on silicon micro-ring resonators," ***Opt. Express*** **15**, 924-929 (2007).

[2] Q. Xu and M. Lipson, "Carrier-induced optical bistability in silicon ring resonators," ***Opt. Lett.*** **31**, 341-343 (2006).

[3] Q. Xu, S. Sandhu, M. L. Povinelli, J. Shakya, S. Fan, and M. Lipson, "Experimental Realization of an On-Chip All-Optical Analogue to Electromagnetically Induced Transparency," *Phys. Rev. Lett.* **96**, 123901 (2006).

[4] Q. Xu, J. Shakya, and M. Lipson, "Direct measurement of tunable optical delays on chip analogue to electromagnetically induced transparency," *Opt. Express*, **14**, 6463-6468 (2006).

[5] Almeida, V. R., Barrios, C. A., Panepucci, R. R., Lipson, M., ***All-optical control of light on a silicon chip***, Nature, pp. 1081-1084 (Oct. 2004).

[6] Almeida, V.R., Barrios, C.A., Panepucci, R.R., Lipson, M., Foster, M.A., Ouzounov, D.G. and Gaeta, A.L., ***All-optical switching on a silicon chip***, Optics Letters, Vol. 29, No. 24, 2867, 15 December 2004.

[7] Koza, J.R. Genetic Programming: On the Programming of Computers by Means of Natural Selection. Cambridge, MA: The MIT Press, 1992.

[8] Crow, James F., and Motoo Kimura. "Efficiency of Truncation Selection." Proceedings of Natl Acad Sci USA 1979, 76:396-399.

[9] Ferreira, Cândida. "Function Finding and the Creation of Numerical Constants in Gene Expression Programming." Advances in Soft Computing – Engineering Design and Manufacturing, Springer-Verlag, 2003: 257-266.